Plasmonics (2017) 12:339–343
DOI 10.1007/s11468-016-0269-3

Wide-Angle Near-Perfect Absorber Based on Sub-Wavelength Dielectric Grating Covered by Continuous Thin Aluminum Film

Minghui Luo[1,2] · Su Shen[1,2] · Yan Ye[1,2] · Yanhua Liu[1,2] · Yun Zhou[1,2] · Linsen Chen[1,2]

Received: 24 February 2016 / Accepted: 9 May 2016 / Published online: 20 June 2016

Abstract We design and numerically investigate an optical absorber consisting of the sub-wavelength dielectric grating covered by continuous thin aluminum film. In this absorber, the aluminum film act as an efficient absorbing material because of the enhanced electric field in the air nano-grooves, and the absorption spect+rum can be manipulated by Fabry-Perot cavity mode resonance. According to the spectrum manipulation mechanism, the wavelength of absorption peak can be tuned by changing the heights and widths of the air nano-grooves. More importantly, the high absorption is very robust to the incident angle around the designed wavelength. From the nanofabrication point of view, the light absorber can be fabricated more easily without the need for ion or electrochemical etching of metal and it is easy to be integrated into complex photonic devices.

Keyword Absorption · Resonance · Grating · Cavity mode

Introduction

Light absorbers have attracted much attention because of their potential applications in photodetectors, solar cells, bolometers, thermal emitters, and plasmonic sensors [1–4]. Perfect absorber with near 100 % absorption in the terahertz region was first reported by Landy et al. in 2008 [5]. Since then, various kinds of structures have been employed to achieve high absorption for a broad range of incident angles, such as multilayer structures [6], metamaterial-based surfaces incorporating metallic nanostructures [5, 7–15]. Using multilayer structures to construct perfect absorbers is a simple method [6]. However, the absorption response is found sensitive to the incident angle. Metamaterial absorbers have been investigated theoretically and experimentally because they can achieve perfect absorption with robust angle-independence over a certain bandwidth [7–10]. The majority of them involve building elaborate metallic patterns on a dielectric spacer film which is attached to a thick metal layer. For these different metallic pattern designs, such as fishnet structure, and cut-wire array, e-beam lithography was the first choice for sample fabrication, which set manufacturing obstacles for the practical applications. In recent years, metallic nanostructures (such as perforated metallic film, strip metallic grating) appear as an inescapable solution for the design and realization of optical nano-antennas able to couple the selective incident optical power with high efficiency [11–15]. Jing Zhang et al. investigated the omnidirectional absorption enhancement in the hybrid system consisting of a gold nanowire array embedded in a slab waveguide [14]. Wenchao Zhou et al. have proposed a nearly perfect polarization-independent and omnidirectional absorber with a metal grating embedded in a lossless dielectric layer atop the metal substrate [15]. However, it is fussy to fabricate discrete metallic nanostructures.

In this paper, we realize a wide-angle near-perfect absorber based on the sub-wavelength dielectric grating covered by continuous thin aluminum (Al) film. The high

✉ Yun Zhou
zyun@suda.edu.cn

✉ Linsen Chen
lschen@suda.edu.cn

[1] College of Physics, Optoelectronics and Energy & Collaborative Innovation Center of Suzhou Nano Science and Technology, Soochow University, Suzhou 215006, China

[2] Key Lab of Advanced Optical Manufacturing Technologies of Jiangsu Province & Key Lab of Modern Optical Technologies of Education Ministry of China, Soochow University, Suzhou 215006, China

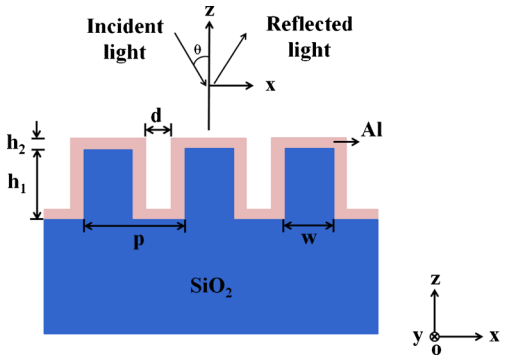

Fig. 1 Schematic of the proposed absorber

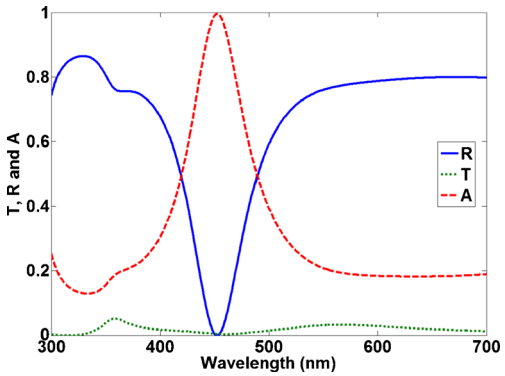

Fig. 2 The simulated absorption, transmission, and reflection spectra for TM polarized light

absorption results from Fabry-Perot cavity modes localized in the air nano-grooves. According to this spectrum manipulation mechanism, the resonance wavelength of absorption can be tuned by changing the height and width of the air nano-grooves. Unlike the absorber incorporating the discrete metallic gratings, our proposed configuration is not composed entirely of aluminum but it consists of SiO_2 grating covered by a thin layer of aluminum. So the proposed absorber can be fabricated more easily without the need for ion or electrochemical etching of metal, and it is easy to be integrated into complex photonic devices, which is an outstanding candidate as high efficiency absorber from the nanofabrication point of view.

Simulation and Discussion

Figure 1 shows the schematic of the absorber, which consists of the dielectric grating covered by continuous Al film. The air nano-grooves were formed between neighboring metal walls. The heights of the air nano-grooves are the same as those of the dielectric grating (h_1). The thickness of the Al layer is h_2. The pitch and the ridge width of the dielectric grating are p and w, respectively. The width of the air nano-groove is d, where $d = p\text{-}w\text{-}2\ h_2$. The dielectric constants of Al are described by the Drude-Lorentz model, and the refractive index of the dielectric grating is set to 1.5 with a negligibly small optical loss [16, 17]. The transverse magnetic (TM) polarized light is obliquely incident from the top at an angle of θ upon the absorber. The absorption is calculated using the rigorous coupled analysis (RCWA) method [18].

Figure 2 presented the simulated absorption, transmission, and reflection spectra at normal incidence ($\theta = 0°$) of the TM polarized light, where $p = 180$ nm, $h_1 = 220$ nm, and $d = 30$ nm. We can observe an absorption peak at 450 nm wavelength with absorption rate large than 99 %. And at the resonance wavelength ($\lambda = 450$ nm), the transmission and the reflection through the structure are almost zero. Therefore, an absorber with near-perfect absorption can be realized with the structure in Fig. 1.

In order to reveal the physical origin of the near-perfect absorption in Fig. 2, we investigated the normalized electromagnetic field distributions at the absorption peak of 450 nm. For TM polarized light, the only three non-zero field components are Ex, Hy, and Ez with a coordinate system O_{xyz} oriented as in Fig. 1. A standing wave pattern in the z-direction is clearly visible in the contour-plots of Ex and Hy. These components are essentially confined in the air nano-grooves. On the contrary, the Ez component is strongly localized around the metallic corners. From Fig. 3b, we can see the magnetic field intensity greatly enhanced in the air nano-grooves. So the air nano-grooves can be regarded as an efficient absorbing material.

For a better understanding of the contribution of the standing wave in the air nano-groove to the near-perfect absorption,

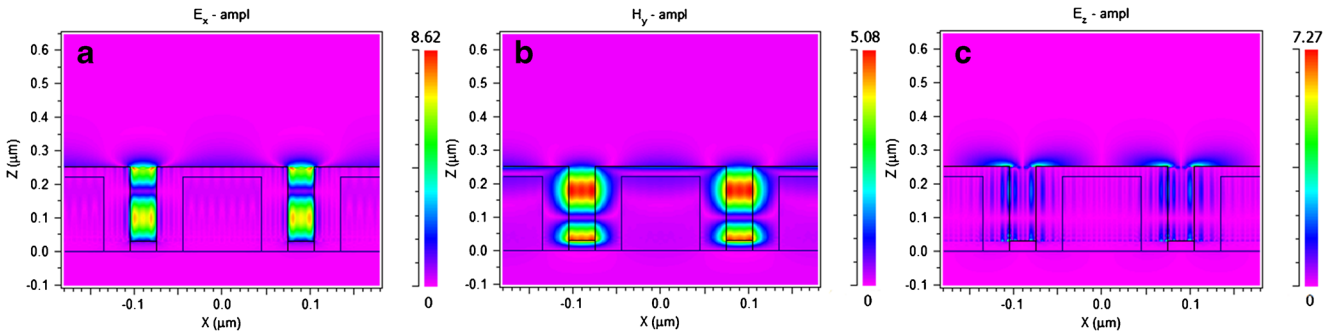

Fig. 3 The calculated Hz field intensity distribution at the resonant peak of 450 nm

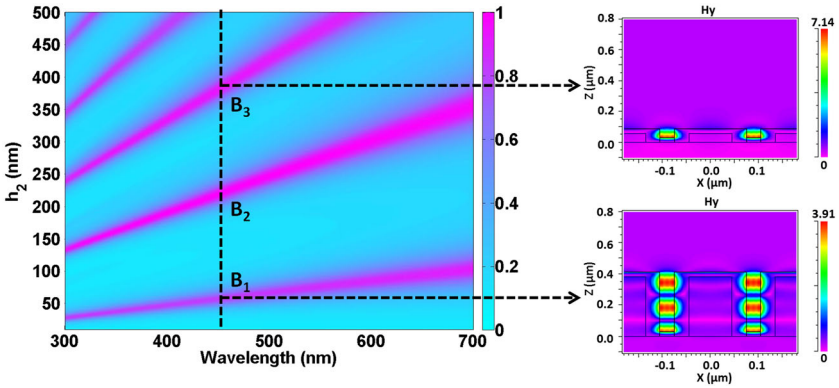

Fig. 4 Dependence of absorbance on air nano-groove heights h_1 for normally incident TM polarized light. The *insets* show the Hy field intensity distribution for incident wavelength 450 nm at point B1 and B3 with grating heights 57 and 380 nm, respectively

we consider a Fabry-Perot (FP) cavity which has two mirrors of finite reflectivity at both ends of the nano-groove [19, 20]. The resonance wavelength at normal incidence is determined by

$$m\lambda + \frac{1}{4}\lambda = n_{\text{eff}} h_1, \quad m = 0, \quad \pm 1, \quad \pm 2, \quad \ldots, \quad \pm N \qquad (1)$$

where h_1 is the height of the air nano-groove, m is positive integer, and n_{eff} is the effective refractive index of the metal-insulator-metal waveguide modes. According to the metal-insulator-metal (MIM) waveguide equation $\sqrt{\varepsilon_d - n_{eff}^2}k_0 d = n\pi + 2\arctan\left(\frac{\varepsilon_d\sqrt{n_{eff}^2-\varepsilon_m}}{\varepsilon_m\sqrt{\varepsilon_d-n_{eff}^2}}\right)$, n_{eff} can be attained. The integer m counts the number of field maximum of the standing wave pattern of Hy. In Fig. 3, these components are plotted for the first excited resonance $m = 1$, under normal incidence ($\theta = 0°$).

From Eq. 1, we can see that the resonance wavelength can be tuned by changing the height (h_1) and the width (d) of the air nano-grooves. In order to verify the absorption characteristics originated from the FP cavity mode, the absorption spectra for different air nano-grooves heights and widths are shown in Figs. 4 and 5, respectively. Figure 4 shows the effect of the air nano-grooves' heights on the absorption behavior by changing h_1 while fixing p and d, where $p = 180$ nm and $d = 30$ nm. As shown in Fig. 4, five bright absorption bands can be observed, and the positions and bandwidths of absorption peaks change with the increase of h_1. The Hy field intensity distributions for the absorption peak at wavelength 450 nm corresponding to point B_1 and B_3 with different grating heights (h_1) 57 and 380 nm are shown in the insets of Fig. 4, respectively. The Hy field intensity distributions of point B_2 with grating height 220 nm have been shown in Fig. 3b. It is clear that standing waves are excited in the air nano-grooves, which confirms the characteristics of the FP cavity mode. As the height (h_1) increases, cavity mode inside the air nano-grooves with different order is excited. The thicker the air nano-grooves' height is, the higher order the cavity mode have. Moreover, the light energy is wholly confined in the air nano-grooves, which leads to the nearly perfect absorption. It is obvious that the absorptive peaks can be designed to appear at particular wavelength by controlling the FP cavity mode resonances in the air nano-grooves. The dependence of absorbance on the widths of the air nano-grooves is shown in Fig. 5. From FP resonance condition (Eq. 1) and MIM waveguide equation, the effective refractive index increases as d decreases, leading to the longer wavelength of the FP resonance. The simulated results in Figs. 4 and 5 demonstrate that the resonance wavelength of absorption can be tuned by changing the heights and widths of the air nano-grooves.

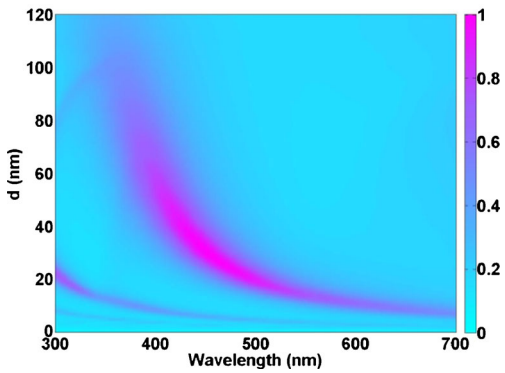

Fig. 5 Absorption versus wavelength and air nano-groove widths for normally incident TM polarized light

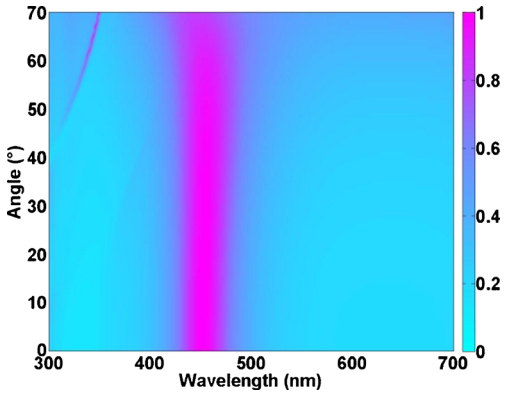

Fig. 6 Absorption spectra as a function of incident angle for the TM polarized light, where $p = 180$ nm, $h_1 = 220$ nm, and $d = 30$ nm

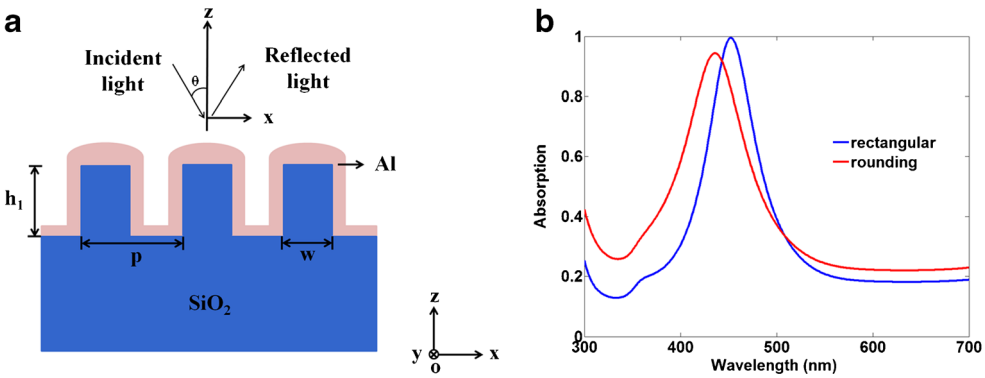

Fig. 7 Schematic of the proposed absorber with the rounding of the borders of the aluminum layer and the simulated absorption spectra

For practical application, the absorber should work over a wide range of incident angle. Figure 6 shows the absorption spectra at various angles of incidence for TM polarization. The bright bands, at which the absorption is maximal, indicate resonance behavior. The absorption approaches nearly 100 % at normal incidence. It is obvious that the peak position does not change, even though the absorptive efficiency gradually decreases from unit to about 91 % with respect to the incident angle θ increasing from 0^o to 60^o. Not only that, the absorptivity can even maintain 81 % at 70^o. The angle-insensitive property of this structure is attributed to the nature of cavity modes [20].

In the actual production process, the metal grating layer can't be rectangular borders, but more rounded corners of the aluminum layer (shown in the Fig. 7a) if the sample is fabricated by direct deposition of aluminum onto a pre-patterned surface. So we discuss the effect of the rounding of the borders of the aluminum layer in Fig. 7b. It is shown that the geometry of the aluminum layer can also determine the resonance wavelength and the absorption efficiency.

Conclusion

In this paper, an optical absorber consisting of the sub-wavelength dielectric grating covered by continuous thin aluminum film for the TM polarized light was analyzed. It can achieve perfect absorption and a good angular tolerance up to 60°. It was demonstrated that the near-perfect absorption can be obtained when the energy related to the FP cavity mode is wholly confined in the air nano-grooves. Well-defined choices of the geometry of the aluminum layer, the heights, and the widths of air nano-grooves allow us to control the resonance performance. From both the structural geometry and the nanofabrication point of view, the optical absorber has a very simple geometrical structure and it is easy to be integrated into complex photonic devices.

Acknowledgments This work was supported by the key Natural Science Foundation of the Higher Education Institutions of Jiangsu Province (grant 14KJB140014, 14KJA510006), by the National Natural Science Foundation of China (NFSC) Major Research Program on Nanomanufacturing (grant No. 91323303), by the NFSC (grant No. 61505134, 61575133, 91023044), the Natural Science Foundation of Jiangsu Province (grant No. BK20140357, BK20140348), the Science and technology project of Suzhou (grant No. ZXG201427, ZXG2013040), the project funded by Soochow University (grant No. SDY2012A18), and the project funded by the Priority Academic Program Development of Jiangsu Higher Education Institutions (PAPD).

References

1. Liu N, Mesch M, Weiss T et al (2010) Infrared perfect absorber and its application as plasmonic sensor. Nano Lett 10(7):2342–2348
2. Zhang B, Zhao Y, Hao Q et al (2011) Polarization-independent dual-band infrared perfect absorber based on a metal-dielectric-metal elliptical nanodisk array. Opt Express 19(16):15221–15228
3. Meng L, Zhao D, Li Q et al (2013) Polarization-sensitive perfect absorbers at near-infrared wavelengths. Opt Express 21(101): A111–A122
4. Cattoni A, Ghenuche P, Haghiri-Gosnet A-M et al (2011) λ3/1000 plasmonic nanocavities for biosensing fabricated by soft UV nanoimprint lithography. Nano Lett 11(9):3557–3563
5. Landy N, Sajuyigbe S, Mock J et al (2008) Perfect metamaterial absorber. Phys Rev Lett 100(20):207402
6. Shu S, Li Z, Li YY (2013) Triple-layer Fabry-Perot absorber with near-perfect absorption in visible and near-infrared regime. Opt Express 21(21):25307–25315
7. Watts CM, Liu X, Padilla WJ (2012) Metamaterial electromagnetic wave absorbers. Adv Mater 24(23):OP98–OP120
8. Shchegolkov DY, Azad A, O'hara J et al (2010) Perfect subwavelength fishnetlike metamaterial-based film terahertz absorbers. Phys Rev B 82(20):205117
9. Ye YQ, Jin Y, He S (2010) Omnidirectional, polarization-insensitive and broadband thin absorber in the terahertz regime. JOSA B 27(3):498–504
10. Hao J, Wang J, Liu X et al (2010) High performance optical absorber based on a plasmonic metamaterial. Appl Phys Lett 96(25): 251104
11. Hu C, Zhao Z, Chen X et al (2009) Realizing near-perfect absorption at visible frequencies. Opt Express 17(13):11039–11044
12. Panoiu NC, Osgood RM Jr (2007) Enhanced optical absorption for photovoltaics via excitation of waveguide and plasmon-polariton modes. Opt Lett 32(19):2825–2827

13. Zhou W, Wu Y, Yu M et al (2013) Extraordinary optical absorption based on guided-mode resonance. Opt Lett 38(24):5393–5396
14. Zhang J, Bai W, Cai L et al (2011) Omnidirectional absorption enhancement in hybrid waveguide-plasmon system. Appl Phys Lett 98(26):261101
15. Zhou W, Li K, Song C et al (2015) Polarization-independent and omnidirectional nearly perfect absorber with ultra-thin 2D subwavelength metal grating in the visible region. Opt Express 23(11):A413–A418
16. Palik ED (1998) Handbook of optical constants of solids. Academic, New York
17. Lumerical Solutions, http://www.lumerical.com
18. Lalanne P, Morris GM (1996) Highly improved convergence of the coupled-wave method for TM polarization. JOSA A 13(4):779–784
19. Liu B, Sun Z (2012) Plasmon resonances in deep nanogrooves of reflective metal gratings. Photonics Nanostruct Fundam Appl 10(1):119–125
20. Shen S, Qiao W, Ye Y et al (2015) Dielectric-based subwavelength metallic meanders for wide-angle band absorbers. Opt Express 23(2):963–970